Zubaidah, T., Korte, M., Mandea, M., Quesnel, Y., Kanata, B., Arumdati, N. (2010): Geomagnetic field anomalies over the Lombok Island region: an attempt to understand the local tectonic changes. - International Journal of Earth Sciences, 99, 5, 1123-1132

DOI: 10.1007/s00531-009-0450-4

Geomagnetic Field Anomalies over the Lombok Island Region: An Attempt to Understand the Local Tectonic Changes

T. Zubaidah

1- Helmholtz Centre Potsdam, Deutsches GeoForschungsZentrum (GFZ), Sektion 2.3 Erdmagnetfeld, Potsdam, Germany

2- Jurusan Teknik Elektro, Fakultas Teknik Universitas Mataram, Indonesia

M. Korte

Helmholtz Centre Potsdam, Deutsches GeoForschungsZentrum (GFZ), Sektion 2.3 Erdmagnetfeld, Potsdam, Germany

M. Mandea

Helmholtz Centre Potsdam, Deutsches GeoForschungsZentrum (GFZ), Sektion 2.3 Erdmagnetfeld, Potsdam, Germany

Y. Quesnel

Helmholtz Centre Potsdam, Deutsches GeoForschungsZentrum (GFZ), Sektion 2.3 Erdmagnetfeld, Potsdam, Germany

Now at

Centre Européen de Recherche et d'Enseignement des Géosciences de l'Environnement (CEREGE), France

B. Kanata

Jurusan Teknik Elektro, Fakultas Teknik Universitas Mataram, Indonesia

Correspondences should be addressed to:

Teti Zubaidah

Helmholtz Centre Potsdam, Deutsches GeoForschungsZentrum (GFZ), Sektion 2.3 Erdmagnetfeld, Raum F-420, Telegrafenberg, 14473 Potsdam, Germany

Tel.: +49-331-288-1233, Fax.: +49-331-288-1235, E-mail: teti@gfz-potsdam.de

"The original publication is available at www.springerlink.com".
Citation: Zubaidah, T., Korte, M., Mandea, M., Quesnel, Y., Kanata, B. (2009 online first) Geomagnetic field anomalies over the Lombok Island region: an attempt to understand the local tectonic changes. *International Journal of Earth Sciences*, doi: 10.1007/s00531-009-0450-4.

Abstract During the last years, several investigations on the earthquakes and related tectonic structures along the Java trench have been conducted. In this study, we focus on the Lombok Island – West Nusa Tenggara (Indonesia), which lies between the centres of the highest intensity of contiguous negative-positive geomagnetic anomalies in this region. The geological and tectonic structures, however, are not known in detail for this island, whereas a better knowledge of these conditions could lead to better estimate the potential earthquake risks and thus a possible improvement of the existing early warning system.

We have performed a ground-based geomagnetic survey at 56 stations in the Lombok Island during October–November 2006 for a detailed mapping and interpretation of geomagnetic anomalies related to the geological and tectonic characteristics. The 2D and 3D magnetic maps show a general geomagnetic anomaly pattern in the Lombok Island which consists of repeated contiguous negative-positive anomalies. Two forward models have been proposed for a profile connecting a strongest apparent dipolar structure. The first model assumes a uniformly magnetized sphere as the source of the anomaly, and could be interpreted as a specific local structure composed by a quite large magnetic body. The second model considers several rocks with different susceptibilities and magnetizations, and could be interpreted as a discontinuity in the geological structures. This model agrees with the local geological surface conditions and the known large scale regional tectonic structure. Therefore, it is used to interpret our results in terms of tectonic characteristics, which suggests the potential existence of a new tectonic element (e.g. a local normal fault) in this region.

Key words: *Geomagnetic field anomaly, Tectonic earthquake, Java Trench, Lombok Island*

1. Introduction

After the 2004 Sumatra earthquake, needs and efforts to assess seismic hazards in the Indonesian region have strongly increased. Several geophysical methods have been proposed to study this region, one of them being the potential field analysis. The relation between the geomagnetic field – in which we are interested – and earthquakes is not obvious, but several recent studies have suggested that magnetic anomalies could help to better understand the geological and tectonic conditions related to seismic activity in the subduction zones.

Purucker and Ishihara (2005) have reported that the present Java subduction zone is evident as a band of negative anomalies situated south and west of Sumatra and Java Islands. Blakely et al. (2005) have suggested that serpentinized magnetic mantle may be common in forearc settings and thus magnetic anomalies may be useful in mapping hydrated mantle in convergent margins. Some studies have indicated that the intense seismic activity could be associated with the subduction in the southern and eastern Indonesian regions. Hinschberger et al. (2005) have proposed a new kinematic model of eastern Indonesia based on a synthesis of geophysical, geological and geochemical studies: the eastern Indonesian region clearly appears as a very active area where the deformation associated to the AUS/PSP/SEA (Australian/Philippine Sea/South-East Asia) triple junction zone is widely distributed and rapidly evoluting. Špičák et al. (2007) have proposed the beginning of a new subduction cycle along the Java Trench, in which the position of Java and Lombok Troughs may be interpreted as a “fossil” trench for the onset of the recently terminating subduction cycle.

In a different direction, piezomagnetic effects have also been considered in relation to earthquakes. Nishida et al. (2007) have explored such effects to analyze precursory and co-seismic signals. While they could not detect significant signals

for the two recent Japanese earthquakes (the 2003 Tokachi-oki of M 8.0 and the 2004 Kushiro-oki of M 7.1, in Hokkaido), they predict effects of several nT for strong earthquakes expected along the Kurile Trench, a region which is also characterized by large amplitudes of geomagnetic anomalies.

Finally, let us note that Balasis and Mandea (2007) have applied wavelet analysis to investigate if electromagnetic disturbances related to the recent great earthquakes could be detected by satellite magnetometers. They have concluded that only a statistical study based on large earthquakes recorded during the CHAMP magnetic mission could bring an answer to such a crucial question. The need for more magnetic measurements in this region is clearly supported by all studies indicated before.

In the following, we focus on the available data over the Lombok Island, the region of interest, from ground to satellite platforms. Let us note that the existence of a large scale contiguous negative-positive high intensity geomagnetic anomaly pattern along the Java trench has been reported in several occasions. Figure 1 shows the total component of the magnetic anomaly over Indonesian region using the magnetic field model MF5 (Maus, et al. 2006) at 5 km altitude. Figure 2 shows a more detailed magnetic anomaly map over the islands along the Java Trench, including the Lombok Island. This map has been generated from cleaned and levelled marine magnetic data available from GEODAS for the interval 1950 - 2004 (Quesnel et al. 2009), combined with marine magnetic data along the Sunda-Banda Arc transition of BGR (Müller and Neben 2006) and aeromagnetic data of AIST and CCOP (Ishihara and Kisimaoto 2002). Figure 1 indicates that the Lombok Island is located between the centres of the highest negative-positive magnetic anomalies in this region, but the detailed map of Fig. 2 can not absolutely support this view, as ground and marine magnetic data are not completely available. Although some preliminary studies were conducted (Zubaidah et al. 2005), no high resolution geomagnetic data are available for the Lombok Island. Due to the lack of state-of-the-art instruments, the quality of some of the first magnetic measurements is questionable for more interpretations.

Our aim is to obtain a comprehensive view of the local conditions of the region by applying some geophysical methods systematically, in order to map and thereafter to interpret in detail the geomagnetic anomalies related to the geological and tectonic structures. Here, we only report on the first results of regional geomagnetic investigations, from new measurements in the field to preliminary interpretations.

2. Geomagnetic survey and data processing

New geomagnetic field measurements on the Lombok Island were done during October–November 2006, by conducting a ground-based magnetic survey of total field intensity at 56 stations, with an average distance between adjacent stations around 2.5 km, as shown in Fig. 3. This survey included measurements at 36 old stations situated in the northern area, which were previously occupied (Zubaidah et al. 2005). Several stations had to be re-located to magnetically more quiet neighbouring places, in order to ensure a higher quality of these measurements. The purpose of the repeated survey is to investigate possible local geomagnetic field anomaly changes, by comparing the recently measured values with the old

ones. We also conducted an additional survey at 20 new stations in the southern area to explore deeper the presumed negative anomaly region. The total geomagnetic field intensity was measured every 30 seconds during 30–60 minutes, using an ENVI PRO Proton Magnetic System (Scintrex), which measures total magnetic fields in the range of 23,000–100,000 nT, with an accuracy of ±1 nT. The measurements noise has been minimized by eliminating those data considered as outliers, based on the percentage of the noise level as recorded by the instrument.

The measured values in a geomagnetic measurement consist of the sum of different field contributions. The so-called internal parts are the core field, also known as the main field, and the lithospheric field, produced by magnetized crustal rocks. The external parts have sources in the ionosphere and magnetosphere. Variations of the external parts also induce currents in the lithosphere and upper mantle resulting in induced secondary fields. Since the external and quickly varying induced fields can reach similar amplitudes as the desired lithospheric signal, they have to be minimized (removed) from measurements. Moreover, the influence of the secular variation, i.e. the slow change of the core magnetic field, has to be taken into account by reducing all measurements to a common epoch.

Based on the assumption that transient variations of geomagnetic field are identical at both the observed stations and the reference station, a simple formulation (Newitt et al. 1997) can be applied to eliminate external field contributions from the measured values (i.e. consider only the internal contributors to obtain geomagnetic mean values of the observed stations), as follows:

$$O(t) - O = C(t) - C,$$

hence

$$O = O(t) - [C(t) - C],$$

where O is the geomagnetic mean value of the observed station; O(t), the instantaneous geomagnetic value measured in the observed station; C(t), the instantaneous geomagnetic value measured in the reference station; and C, the geomagnetic mean value of the reference station.

Following the above formulation, continuous field readings from a nearby reference station are necessary for this data processing. Two Base Stations have been set up consecutively for this purpose, one for the southern area (BS-1) and one for the northern area (BS-5). Unfortunately, the second Base Station was destroyed on the second day of the second part of our survey. Therefore, for the northern area, we had to choose and to use the minute magnetic data provided by one of the three neighbouring geomagnetic observatories – Tondano (TND), Kupang (KPG) and Kakadu (KDU) – as the reference station for data reduction processing.

The evaluation of the suitability of the data provided by the three neighbouring geomagnetic observatories has been done by comparing them with corresponding variations recorded continuously during 16 days in the Penyu Island (PNY), a tiny and magnetically quiet island located very close (about 1.5 km) to the Lombok Island. An Overhauser magnetometer (GSM-19 v7.0, GEM System), measuring

total magnetic fields ranged 15,000–120,000 nT with an accuracy of ±0.1 nT, was installed on PNY as well as on BS-1 and BS-5. This instrument was verified by comparing its reading with the NGK (Niemegk geomagnetic observatory, Germany) standard Overhauser magnetometer. Moreover, the Proton magnetometer (ENVI PRO) used at the stations was calibrated to this Overhauser magnetometer, via cross-reading at the Calibration Stations (Calib). The locations of three neighbouring observatories, the Penyu Island, the Calibration Stations, and two Base Stations are shown in Fig. 1 and Fig. 3.

Data provided by TND turned out not to be suitable, because of significantly larger diurnal variation (about 36 nT between day and night time), probably due to its location closer to the magnetic equator. Data provided by KPG, which is the nearest observatory (about 850 km East of the Lombok Island), are actually of the best quality, but unfortunately, because of some technical problems they are not available for some days of our magnetic survey. Consequently, we chose the KDU data, which are in good agreement with PNY, to eliminate the external field contributions on the observed stations data. All measurements have been reduced to epoch 2006.84, which is November 1st 2006, a date near the middle of the survey time-span.

After the mean values for each station have been calculated, the data were classified by using the standard deviation (*StDev*) values, following the criteria: good quality (*StDev* < 2 nT), intermediate (2 nT ≤ *StDev* < 5 nT), and low quality (*StDev* ≥ 5 nT) data. The next step in the data processing was to choose more reliable data, when there were redundant measurements at the same station on different days. In this case, the observations that were made during more magnetically quiet days, i.e. on the day when the *Kp* index (http://www.gfz-potsdam.de/pb2/pb23/GeoMag/niemegk/kp_index/index.html) and *K* indices for the Australian observatories (http://www.ips.gov.au) are smaller than 3, have been kept.

By using only good quality data and subtracting the 10th generation IGRF values (Maus et al. 2005) to eliminate the core field, a 2D geomagnetic anomaly map has been generated using Oasis montaj 6.4 (Geosoft software). To obtain it, the Kriging method has been applied, using linear power model with a blanking radius of 0.0527° (equal to 5.85 km) to interpolate the available data and to show the empty spaces for the parts without data, as shown in Fig. 3. This figure shows a strong dipolar magnetic anomaly in the southern part of the survey area, with the minimum point located on (-8.76°N, 116.03°E) and the maximum point on (-8.73°N, 116.09°E). The new values of the geomagnetic anomaly are lower compared to the 2004–2005 survey results with the differences ranging from -239.26 to -2941.80 nT. These differences are larger than reasonable decreases of an induced anomaly due to the main field in this region, characterized by a secular variation of some -13 nT/year. However, we have to stress once more that the previous measurements have to be taken with care because of the large uncertainties in the observations. Therefore, these differences are not discussed further here, but will be investigated in a future work when survey data from fall 2007 to spring 2008 will be available.

Furthermore, by generating a 3D view as shown in Fig. 4, the horizontal gradient as well as geomagnetic anomaly pattern in the Lombok Island could be described as repeated contiguous negative-positive anomalies: a low anomaly in the north, a high positive anomaly in the middle, and a negative anomaly in the south. If the

negative anomaly extends southward, then it matches the above mentioned general geomagnetic anomaly pattern along the Java Trench (see Fig. 2). This ensures its reliability and promises a smooth transition to the global geomagnetic data (see Fig. 1).

3. Models and interpretations

By extracting a profile, connecting the strongest apparent dipolar magnetic anomaly from the negative part on (-8.79°N, 115.98°E) to the positive part on (-8.70°N, 116.16°E), as illustrated by a blue straight line on Fig. 3 and by a black curve on Fig. 4, two forward models have been constructed.

The first model only assumes one uniformly magnetized sphere, equivalent to a dipole (Blakely 1995). In this modelling, location and magnetization parameters have been adjusted (individually and together) using a discrete exploration procedure to predict the magnetic anomaly along the profile. Seven parameters have been investigated: the horizontal coordinates (x, y), the depth (z), the radius (r), the magnetization intensity (M), inclination (I) and declination (D). Parameters ranges are indicated in Table 1. We have arbitrarily constrained the source to be along the profile (i.e. -8.8°N $\leq y \leq$ -8.7°N; with sampling interval (denoted thereafter as *si*) of 0.1°) and within the longitudinal extent of the anomaly (116.00°E $\leq x \leq$ 116.13°E; with *si* of 0.01°). Then, the radius of the sphere is considered exclusively smaller than the depth of its center ($r < z$), and z is limited to a maximum 20 km, because the resolution of the used data prevents to map very deep crustal sources. Nevertheless, characterizing the depth with high accuracy is needed. Therefore, *si* of 0.1 km between 0 and 20 km is used for the depth, and *si* of 0.5 km for the radius. Concerning magnetization parameters, the intensity is investigated using *si* of 1 Am^{-1} between 0 and 20 Am^{-1}. This allows us to cover a wide range of rock magnetized susceptibility values. Magnetization directions are first forced to be aligned with the main magnetic field directions in the corresponding area for the survey epoch, i.e. I_{if} = -34.75°and D_{if} = 1.70° (http://ngdc.noaa.gov/geomagmodels/IGRFWMM.jsp). However, it appears that assuming an induced magnetic source does not show a good fit of the magnetic anomaly, whatever the remaining parameters are. Therefore, we have also used a discrete exploration of inclination (-90° $\leq I \leq$ 90°; *si*: 2°) and declination (-180° $\leq D \leq$ 180°; *si*: 15°) values.

Figure 5 shows the best fit model obtained via this approach, and its parameters are indicated in Table 1. This magnetic body is located in the upper-middle crust and has an intense magnetization, with inclination and declination far from the induced directions. With this geometry, the source of the anomaly would have to have a very strong remanent magnetization. This result is in a good agreement with the previous interpretation (Zubaidah et al. 2005). However, the new model suggests a shift of the structure location to the southwest direction and a relatively smaller size of the body.

The second model was obtained using the GM-SYS Profile Modeling (an extension to Oasis montaj, Geosoft software), which assumes rocks and sediments, as several blocks having different susceptibilities and remanent magnetizations, as the sources of anomalies. In this modelling method, the general shape of the total anomaly response signal is determined primarily by locations

and shapes of each block, whereas detailed curvature and its amplitude are influenced by the susceptibilities and the remanence parameters (magnetization intensity, inclination, and declination) of each block.

To start our model, the observed magnetic anomaly signals have been directly imported from the concerned magnetic grid by digitizing the desired profile on the 2D anomaly map of Fig. 3, taking 225 points to get about 100 m intervals between adjacent points. The Earth's surface shape has been derived from the topography grid of SRTM30 Plus v4, obtained from the Geosoft DAP server (http://dap.geosoft.com/geodap/home/default.aspx). The structures of surficial rocks as well as their subsurface continuations have been determined from the local geological map (Mangga et al. 1994), whereas deeper structures have been estimated based on the seismic and geoacoustic investigations over the closest area (the 116° corridor of Kopp and Flueh 2007). To resolve uncertainties of geological structures across the coastal area, the geological profile (green lines of Fig. 3 and Fig. 7) has been shifted 1.5 km south-eastward (landward) from the anomaly profile (blue lines of Fig. 3 and Fig. 7).

To get proper calculations, several initial parameters of the ambient core magnetic field have to be given, including its magnitude (*H*), inclination (*FI*), and declination (*FD*); additionally the profile azimuth and the relative strike angle have also to be set. All initial magnetic parameters are determined from the 10^{th} IGRF for the location of the south Base Station (http://ngdc.noaa.gov/geomagmodels/IGRFWMM.jsp), while profile azimuth could be determined from the direction of the extracted profile counted clockwise from the true North. The strike angle is set to 70° relative to the extracted profile, considering the known nearest surface lineament on the geological map, which shows a south-eastward trend. The red lines of Fig. 3 and Fig. 7 show the intended strike line. All the initial parameter inputs of the second model are indicated in Table 2.

Firstly, an intrusive igneous rock (labelled as *Tmi* on Fig. 6 as well as on the geological map of Fig. 7), due to its extremely high susceptibility, has been assumed as the main source of anomalies. We have started our model by taking a simple subsurface continuation of this block (directed straight downward to the basement rocks), also by simply determining its inclination and declination initially in line with the ambient magnetic field. Based on the local geological map, it has been considered that this intrusion is composed by Dacites and Basalts. To produce such a huge anomaly, the initial susceptibility should be close to the maximum value of basaltic rocks (ranged 250–180,000 x 10^{-6} SI (Table 1 of Hunt et al. 1995)), while the remanent magnetization has to be relatively low and in the permissible range of Koenigsberger ratio (*Qn*) of intrusive rocks (ranged 0.1–20 (Table 6 of Hunt et al. 1995)). We have then tried to adjust the inclination and declination values, in combination with magnetization intensity, to get the desirable response. Changes of the declination only affect the anomaly amplitudes and have no effects on the shape of the response signal. Therefore we keep the initial value of declination. Changes in the inclination of the magnetization only affect the response signal on the right side of the block. In other words, the negative part of the anomaly signal could only be fit by shifting the block to the left (as seen in the dark blue curve of Fig. 6), and getting a significant decrease of the RMS error (from initially 349.18 nT down to about 150 nT).

To improve the fit to the anomaly signal, contributions of other nearby rocks have to be taken into account. Volcanic rocks typically have strong remanent magnetization. After looking back at the geological map, we have modelled two blocks of volcanic rocks on both sides of the intrusive rocks, labelled as *TompR* and *TompL* on Fig. 6, representative of surrounding volcanic rocks (labelled as *Tomp* on the geological map of Fig. 7). For these blocks, we take rather low values of susceptibility (i.e. 1,000 x 10^{-6} SI) and relatively high values of remanent magnetization intensity, but still keep the relationship between both values in the permissible range of Koenigsberger ratio (*Qn*) of volcanic rocks (ranged 30–50 (Table 6 of Hunt et al. 1995)). Their inclinations then have to be adjusted to a value which provides the lowest error; let us note that both inclinations must be equal, regarding the same age of their geological formations.

With the above described approaches, the total response shape (black curve of Fig. 6) already agrees with the observed curvature (black points of Fig. 6). At this step, the RMS error has been reduced to about 120 nT, without reaching yet our suitable limitation of misfit. We expect that the RMS error would be less than 5% of the peak to peak anomaly (i.e. about 60 nT), which substantially reduces the range of possible solutions, and can provide a reasonably reliable model.

Then, adjustments of the lowest ends of both volcanic blocks (their lowest boundaries to the lower sedimentary rocks) lead to significantly reduce the errors. Further decreasing of errors could be reached by introducing lateral extensions of the intrusive rock, representing the sills on the left and right sides (labelled as *Tmi-extL* and *Tmi-extR* on Fig. 6). The possible occurrence of such sills is supported by the geological map of Fig. 7, regarding the occurrence of many small intrusions in the surroundings.

After applying those approaches, we actually have reduced the RMS error to about 80 nT, close to the expectation, but still have considerably bothersome ripples at both peaks of negative and positive anomalies. Although they are below the possible resolution given by our measurement station density, we aim for a smoother response of the negative anomaly. Therefore we have considered the contribution of a surficial sedimentary rock (labelled as *Tomk* on Fig. 6 as well as on the geological map of Fig. 7), which had been underestimated before. This block, as described by the geological map, could be considered as Sandstone with mean susceptibility value of about 10,000 x 10^{-6} SI (Table 1 of Hunt et al. 1995). Its inclination and declination is assumed to be the same as those of volcanic rocks (*TompL* and *TompR*), due to the same age of their geological formations. By adjusting its remanent magnetization intensity in the permissible range of Koenigsberger ratio (*Qn*) of average sedimentary rocks (ranged 0.02–10 (Table 6 of Hunt et al. 1995)), we have achieved a smooth negative anomaly peak. Table 3 indicates magnetic properties of all rocks used for the second model. Finally, carefully adjusting the detail shapes of intrusive rock, as well as its right side bounding to the volcanic rock, leads to much better smoothness of the positive anomaly peak, hence reducing the RMS error to the very low value of about 35.5 nT (see red curve of Fig. 6).

Let us suggest a possible interpretation of the second model in terms of tectonics. The intrusive rock formations on the Lombok Island might be caused by the subduction processes on the Java Trench, about 315 km south of the block considered for the studied geomagnetic anomaly (Kopp and Flueh 2007). On this convergent margin, the Australian plate subducts beneath the Eurasian plate, resulting in compressional faults with directions normal to the Java Trench (Kopp

et al. 2006). Moreover, from the best documented tectonic regime for the Lombok Island and circumference regions (segment 3 in Fig. 7 of Špičák et al. 2007), all 19 earthquake events in 1977 show normal faulting (no strike-slip) with very homogeneous position of nodal planes parallel to the trench. In the second model, we can infer a possible tectonic interpretation from the differences of the depth extensions of the volcanic rocks, with the left block reaching about 0.5 km deeper than the right one. The volcanic rocks (i.e. the oldest formation on the Lombok Island, which formed in the Late Oligocene to Early Miocene) can be assumed to be a direct product of the Java Trench subduction, and therefore initially a single continuous structure. Discontinuities in the local geological structures occurred later, by intruded igneous rock in the Middle Miocene, as a result of a continued subduction on this region. Here, a subsurface normal faulting could be assumed, regarding the relationship between volcanic rocks on the left side (*TompL* of Fig. 6) and the volcanic rocks on the right side (*TompR* of Fig. 6), corresponding to the hanging wall and the footwall (i.e. *TompL* moves downward relative to *TompR*).

Finally, we summarize that the second model suggests the possible existence of a subsurface normal fault in this region, which might be considered as a potential trigger for local tectonic earthquakes. This interpretation agrees well with the known regional geological and tectonic structures. As shown in the geological map of Fig. 7, the boundary between the negative and positive part of geomagnetic anomaly (red lines of Fig. 3 and Fig. 7), also considered as the strike direction of the suspected fault line in our model, is parallel to the known nearest surface lineament.

4. Discussions and Conclusions

The general geomagnetic anomaly pattern in the Lombok Island consists of repeated contiguous negative-positive anomalies. A strong dipolar magnetic anomaly in the south could be interpreted in two different ways: as a specific local structure composed by a quite large magnetic body or as a discontinuity in the geological structure (e.g. potentially local fault). The second proposed model and its interpretation are supported by the agreement with the known large scale regional tectonic structure and local geological surface conditions. This model seems to be the more reasonably explanation for the observed magnetic anomaly, and suggests a possible association with geological and tectonic features in this area.

We have presented the first detailed images of the magnetic field over a part of the Lombok Island as an initial step to obtain a better understanding of the geological and tectonic structures. Our preliminary modelling results show the capability of magnetic ground survey data to underline new tectonic elements (e.g. the local faults), which, however, should be further confirmed by other studies. Although MT (magneto-telluric) measurements are preferable to investigate electrical conductivity of Earth's rocks and sediments, it would be very difficult to conduct such measurements appropriately, due to topographical constraints over the Lombok Island and very dense population at some places. DC resistivity measurements are, therefore, expected to provide complementary information.

Moreover, because the significant magnetic anomaly in this island is an intriguing one, recently (during fall 2007 and spring 2008) new scalar geomagnetic

measurements have been conducted over a broader area of the Lombok Island. Our aim is to cover not only the subduction zone in the South (the Java Trench), but also the volcanic area (Mount Rinjani) and the zone of possible subduction extension and reactivation in the North (the Flores Thrust). Figure 2 shows the locations of the main concerned tectonic settings of this region. At the time of writing, these measurements are in the processing stage. Let us note that we would like to connect our results to the existing eastern Asian anomaly map and extend our investigated area. Furthermore, we plan to install some continuous geomagnetic measuring instruments permanently on the Lombok Island. This observatory, planned to record the total field intensity as well as three components of the geomagnetic field, will be a very valuable complement for the next magnetic surveys.

Acknowledgements We would like to address our appreciations to the reviewers and editors for very constructive comments and suggestions. We thanks to Muhammad Husni and Hendar Gunawan (BMG, Indonesia) for providing the Tondano geomagnetic observatory data; K. Yumoto and Shuji Abe (SERC, Kyushu University, Japan) for providing the MAGDAS Kupang data. C. Subarya, Hery Hardjono and Awang H. Satyana have provided us with fruitful discussions about tectonics of Indonesia, Naila Mohamed Babiker about seismicity, and Mohamed Hamoudi about magnetic modelling. Special thanks for Seiya Uyeda and K. I. Oyama for their interests and comments on our first public speaking during the International Workshop on Seismo-Electromagnetic Phenomena (IWSEP) 2007 in Bandung. For our successful field research, we also gratefully thanks to all family and friends, Sekotong people, the members of the research team of Electrical Engineering Dept. of Mataram University, Institut Teknologi Bandung (ITB), and Institut Teknologi Sepuluh Nopember (ITS) Surabaya, especially for the best co-operation of Widya Utama and D.D. Warnana.

References

Balasis G, Mandea M (2007) Can electromagnetic disturbances related to the recent great earthquakes be detected by satellite magnetometers? *Tectonophysics* 431:173-195.

Blakely RJ (1995) Potential theory in gravity and magnetic applications. Cambridge University Press, Cambridge.

Blakely RJ, Brocher TM, Wells RE (2005) Subduction-zone magnetic anomalies and implications for hydrated forearc mantle. *Geology* 33(6):445-448.

Hinschberger F, Malod JA, Rehault JP, Villeneuve M, Royer JV, Burhanuddin S (2005) Late Cenozoic geodynamic evolution of eastern Indonesia. *Tectonophysics* 404:91-118.

Hunt CP, Moskowitz BM, Banerjee SK (1995) Magnetic properties of rocks and minerals. In: Ahrens TJ (ed) Rock physics & phase relations, Handbook of physical constants. American Geophysical Union, Washington, pp 189-204.

Ishihara T, Kisimaoto K (2002) Magnetic Anomaly Map of East Asia 1:4,000,000, CD-ROM Version (2nd Edition), Digital Geoscience Map P-3, Geological Survey of Japan (AIST) and Coordinating Committee for Coastal and Offshore Geoscience Programmes in East and Southeast Asia (CCOP).

Kopp H, Flueh ER, Petersen CJ, Weinrebe W, Wittwer A, Meramex Scientists (2006) The Java margin revisited: Evidence for subduction erosion off Java. Earth Planet Sci Lett 242:130-142.

Kopp H, Flueh ER (2007) Seismic and geoacoustic investigations along the Sunda-Banda Arc transition. FS Sonne Fahrtbericht/Cruise Report SO 190 SINDBAD, Report Nr. 8, IFM-GEOMAR, Leibniz-Institut für Meerewissenschaften an der Universität Kiel.

Mangga SA, Atmawinata S, Hermanto B, Amin TC (1994) Geologi lembar Lombok, Nusatenggara, Lembar 1807, Pusat Penelitian dan Pengembangan Geologi, Indonesia.

Maus S, Macmillan S, Chernova T, Choi S, Dater D, Golovkov V, Lesur V, Lowes F, Lühr H, Mai W, McLean S, Olsen N, Rother M, Sabaka T, Thomson A, Zvereva T (2005) The 10th generation international geomagnetic reference field. *Phys Earth Planet Inter* 151:320-322.

Maus S, Rother M, Hemant K, Stolle C, Lühr H, Kuvshinov A, Olsen N (2006) Earth's lithospheric magnetic field determined to spherical harmonic degree 90 from CHAMP satellite measurements. *Geophys J Int* 164:319-330.

Müller C, Neben S (2006) Research Cruise SO190 Leg 1, Seismic and geoacoustic investigations along the Sunda-Banda Arc transition, with RV Sonne. Cruise report and preliminary results, Bundesanstalt für Geowissenschaften und Rohstoffe (BGR), Hannover.

Newitt LR, Barton CE, Bitterly J (1997) IAGA Guide for Magnetic Repeat Station Surveys.

Nishida Y, Utsugi M, Mogi T (2007) Tectonomagnetic study in the eastern part of Hokkaido, NE Japan (II): Magnetic fields related with the 2003 Tokachi-oki earthquake and the 2004 Kushiro-oki earthquake. *EPS* 59:1181–1186.

Purucker M, Ishihara T (2005) Magnetic images of the Sumatra region crust. EOS 86(10):101-102.

Quesnel Y, Catalan M, Ishihara T (2009) A new global marine magnetic anomaly data set. J. *Geophys. Res.* Doi:10.1029/2008JB006144.

Špičák A, Hanuš V, Vaněk J (2007) Earthquake occurrence along the Java trench in front of the onset of the Wadati-Benioff zone: Beginning of a new subduction cycle? *Tectonics* 26:TC1005.

Zubaidah T, Kanata B, Utama W, Warnana DD, Arumdati N (2005) Laporan akhir penelitian - PRSD MIPA tahun 2005. Laporan penelitian, Jurusan Elektro Fakultas Teknik-Universitas Mataram.

Table 1. Parameters used for *the first* model

Parameter	Range	Best fit
Coordinate (x)	116.00°E ≤ x ≤ 116.13°E; *si*: 0.1°	116.07°E
Coordinate (y)	-8.8°N ≤ y ≤ -8.7°N; *si*: 0.01°	-8.74°N
Depth (z)	0 ≤ z ≤ 20 km; *si*: 0.1 km	6.5 km
Radius (r)	0 ≤ r ≤ 20 km; *si*: 0.5 km	3.5 km
Magnetization intensity (M)	0 ≤ M ≤ 20 Am^{-1}; *si*: 1 Am^{-1}	14 Am^{-1}
Inclination (I)	-90° ≤ I ≤ 90°; *si*: 2°	0°
Declination (D)	-180° ≤ D ≤ 180°; *si*: 15°	-113°

Table 2. Initial parameters used for *the second* model

Parameter	Initial value
Earth's magnetic field: Magnitude [Am^{-1}]	36.095 (equal to 45358.4 nT)
Inclination [deg]	-34.75
Declination [deg]	1.70
Profile azimuth [deg]	68.2
Relative strike angle [deg]	70

Table 3. Magnetic properties of rocks used for *the second* model

Block's name	Susceptibility [10^{-6} SI]	Remanence Magnetization		
		Intensity [Am^{-1}]	Inclination [deg]	Declination [deg]
Intrusive igneous rock (*Tmi*)	110,000	0.4	52	1.7
Volcanic rock (*TompL*)	1,000	1.2	17	1.7
Volcanic rock (*TompR*)	1,000	1.2	17	1.7
Intrusive igneous rock (*Tmi-extL*)	110,000	0.4	52	1.7
Intrusive igneous rock (*Tmi-extR*)	110,000	0.4	52	1.7
Sedimentary rock (*Tomk*)	10,000	1.0	17	1.7

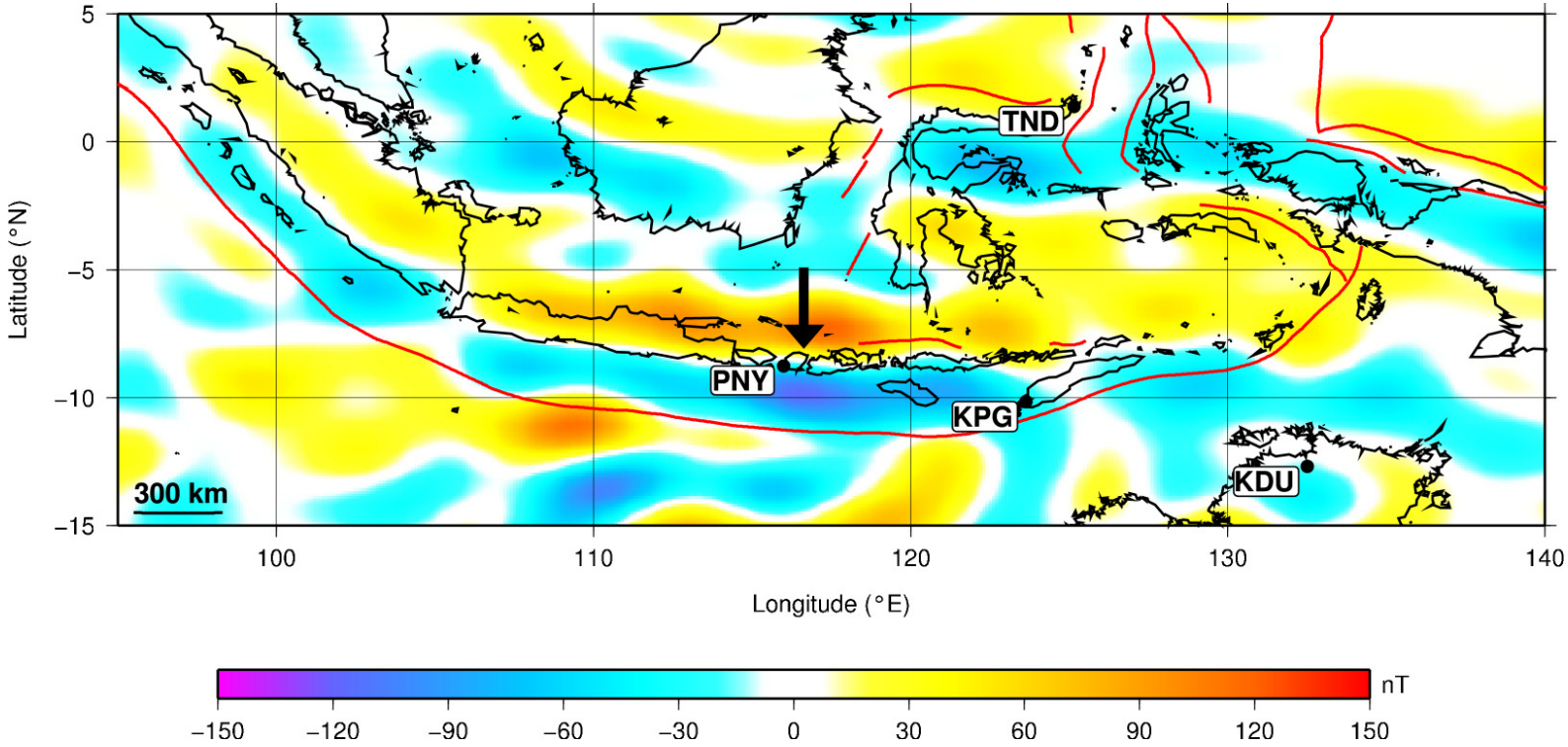

Figure 1. Map of the total component of the large-scale lithospheric field for Indonesian region obtained from the MF5 model (Maus, et al. 2006) at 5 km altitude. Plate boundaries and subduction zones are indicated as red lines. The Lombok Island (pointed out by a black arrow) is located between the highest intensity contiguous negative-positive geomagnetic anomalies in this region. Black circles are the locations of the Penyu Island (PNY) and three neighbouring geomagnetic observatories, i.e. Tondano (TND), Kupang (KPG), and Kakadu (KDU).

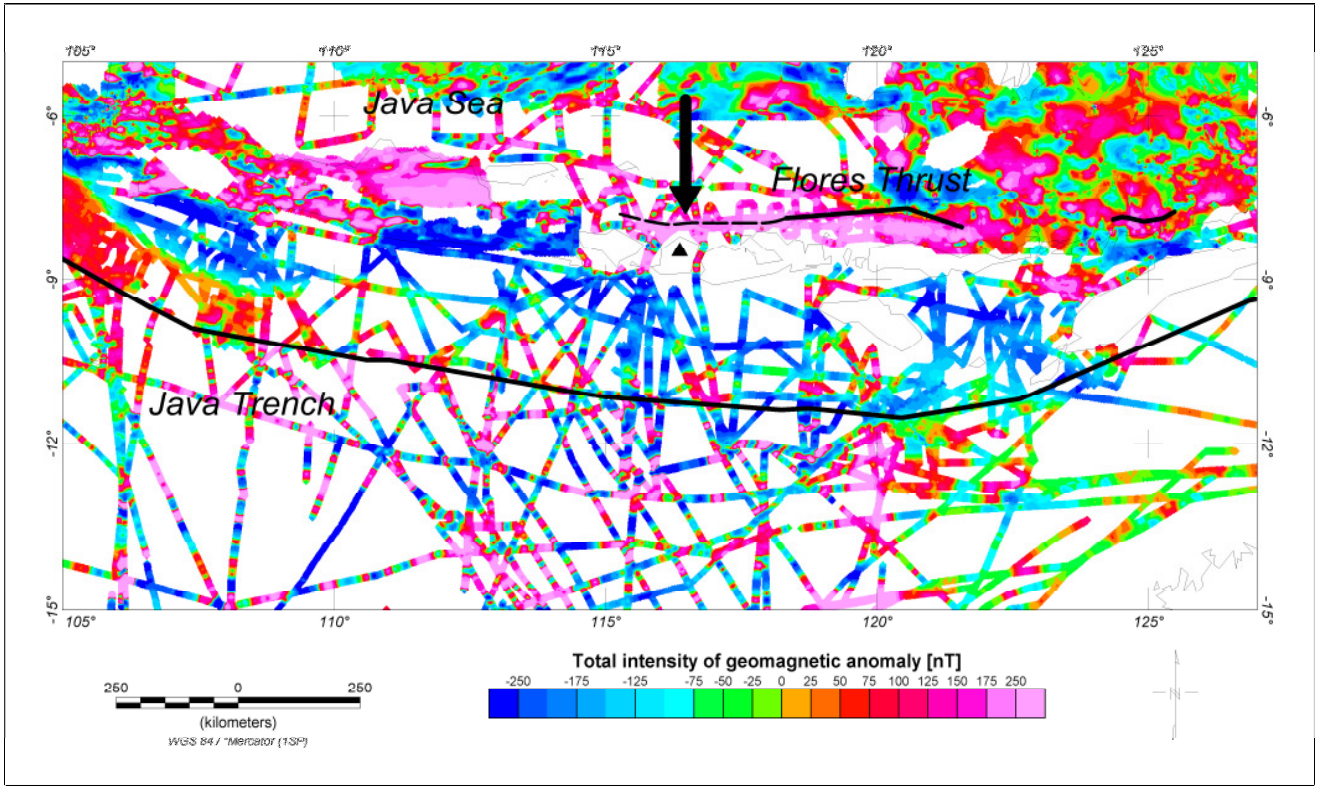

Figure 2. Detailed map of the total field anomaly for southern part of Indonesian region: a contiguous negative-positive anomaly pattern clearly exists along the Java Trench. The position of the Lombok Island is pointed out by a black arrow, while the black triangle represents the location of Mount Rinjani. The subduction zones are indicated as black solid lines, while the dashed one indicates its presumed extension. This map is generated from cleaned and levelled marine magnetic data available from GEODAS for the interval 1950–2004 (Quesnel et al. 2009), combined with marine magnetic data along the Sunda-Banda Arc transition of BGR (Müller and Neben 2006) and aeromagnetic data of AIST and CCOP (Ishihara and Kisimaoto 2002). The white areas over oceans or islands, including that over the Lombok Island, indicate that no data are available.

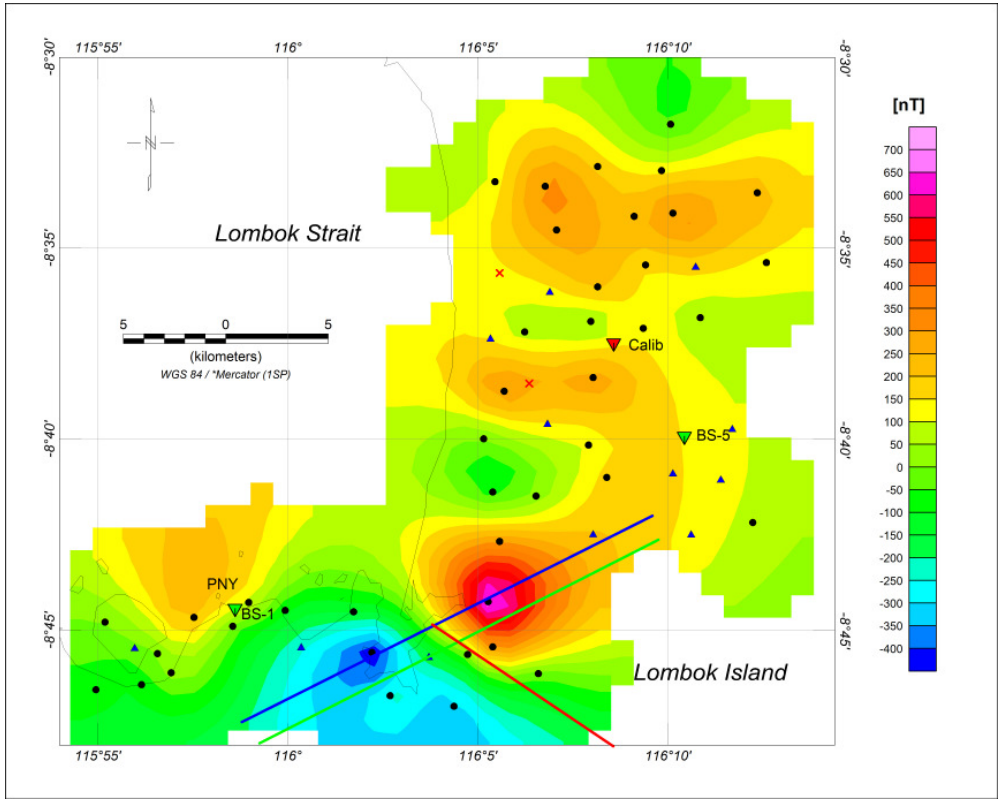

Figure 3. Map of the geomagnetic total field anomaly interpolated over the surveyed area on the Lombok Island. The two base station locations are shown as green inverted triangles, while the Calibration Stations is depicted as a red inverted triangle. The exact location of the Penyu Island is marked with PNY. The geomagnetic survey stations are also shown, providing good quality (black points), intermediate (blue triangles) and low quality (red crosses) data (see text for more details). Only the data with good quality are used. The blue line represents the trace of the magnetic profile studied in the following, which connects two peaks of a strongest apparent dipolar magnetic anomaly. The green line represents the trace of the geological profile used in *the second* model, while the red one represents the presumed strike direction.

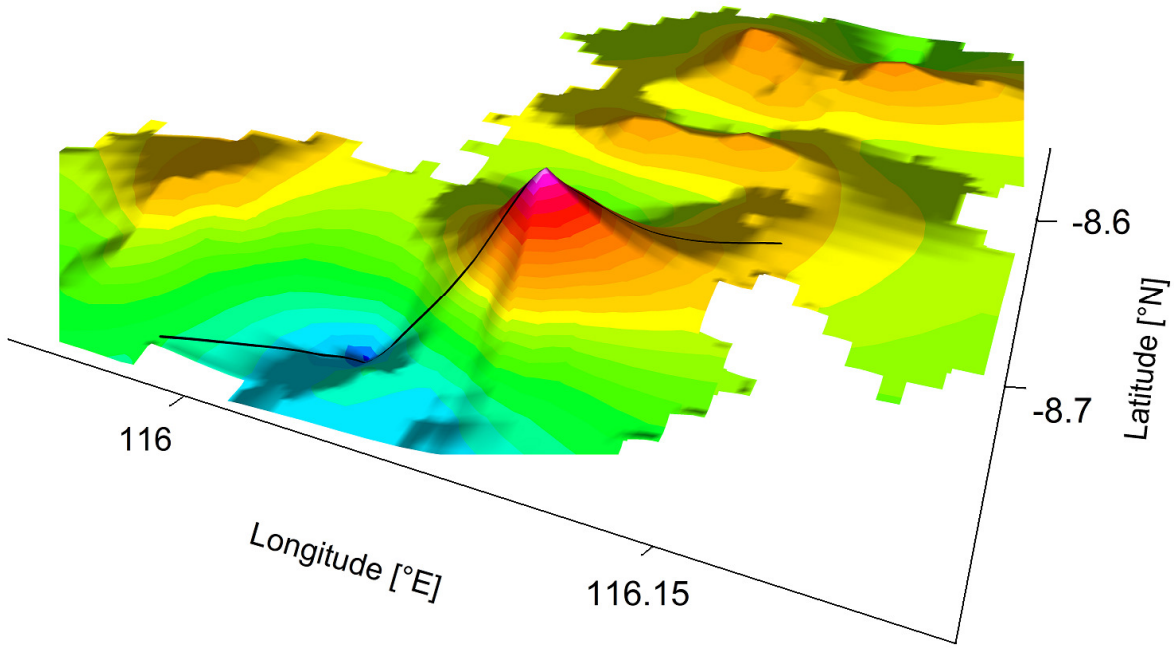

Figure 4. 3D view of the geomagnetic total field anomaly map for the same area as in **Fig. 3**, underlining the repeated contiguous negative-positive anomalies. The intensities of the geomagnetic anomalies are contoured in the form of elevations and leveled with colour scale exactly as in **Fig. 3**. The black curve represents the trace of the magnetic profile studied in the following, which connects two peaks of a strongest apparent dipolar magnetic anomaly.

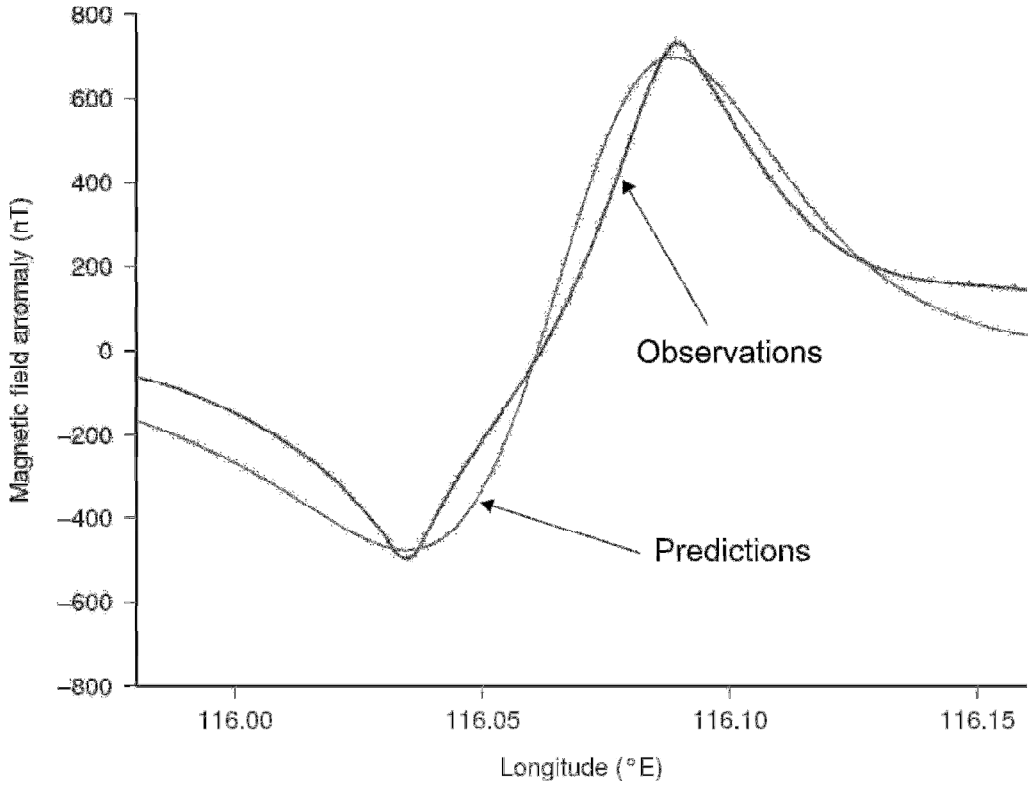

Figure 5. Comparison between *the first* forward model (thin line) that assumes a uniformly magnetized sphere as the source of the anomaly and the profile of observations (thick line).

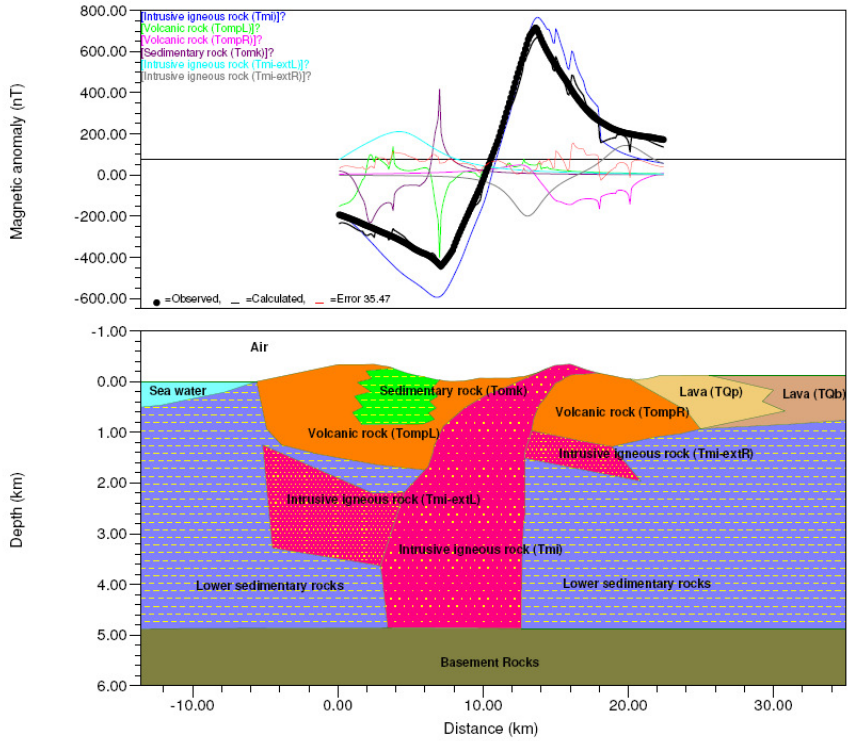

Figure 6. Comparison between *the second* forward modelled profile (black line on top panel) and the profile of observations (black dots on top panel). The individual responses of the blocks could be seen as the colour legend on the left top of top panel, while the errors are represented by the red line. This model assumes rocks and sediments (as several blocks having different susceptibilities and remanent magnetizations) as the sources of anomalies, obtained by using the GM-SYS Profile Modeling (an extension to Oasis montaj, Geosoft software).

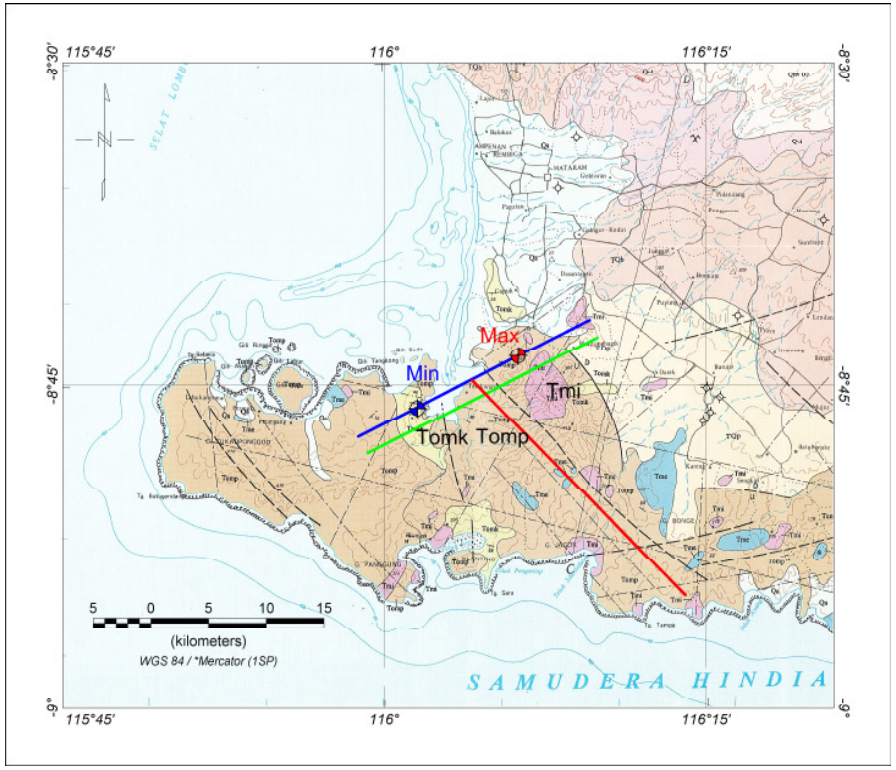

Figure 7. The geological map of corresponding area (Mangga, et al., 1994.) shows the geological formations which have contribution to the geomagnetic anomaly: Intrusive igneous rock (*Tmi*), Volcanic rock (*Tomp*), and Sedimentary rock (*Tomk*). The blue line indicates the location of the extracted profile of **Fig. 3** and **Fig. 4**, while the green line represents the trace of the geological profile used in *the second* model. The exact positions of two peaks of anomaly are shown as cross circled symbols, labelled as *Min* (for the peak of the negative anomaly) and *Max* (for the positive one). The red line, representing the boundary between the negative and positive parts of the studied geomagnetic anomaly, considered also as the strike direction of the suspected fault line in *the second* forward modelling, is parallel to the known nearest surface lineament.